MEASUREMENT OF OXYGEN CONTENT OF URANIUM OXIDE FUEL AND STEEL

C. E. Calado, E. L. Machado and
L. Holland

PUBLICAÇÃO IEA 425 CEN 45	AGOSTO/1976

PUBL IEA 425
CEN 45

AGOSTO/1976

MEASUREMENT OF OXYGEN CONTENT OF URANIUM OXIDE FUEL AND STEEL

C.E Calado, E L. Machado and

L Holland

COORDENADORIA DE ENGENHARIA NUCLEAR
(CEN)

INSTITUTO DE ENERGIA ATOMICA
SÃO PAULO – BRASIL

APROVADO PARA PUBLICAÇÃO EM FEVEREIRO/1976.

INSTITUTO DE ENERGIA ATÔMICA
Caixa Postal 11.049 (Pinheiros)
Cidade Universitária "Armando de Salles Oliveira"
SÃO PAULO – BRASIL

NOTA: Este trabalho foi conferido pelo autor depois de composto e sua redação está conforme o original, sem qualquer correção ou mudança.

TABLE OF CONTENTS

LIST OF TABLES

LIST OF FIGURES

MEASUREMENT OF OXYGEN CONTENT OF URANIUM OXIDE FUEL AND STEEL

C. E. Calado, E. L. Machado and
L. Holland

ABSTRACT

Quantitative oxygen analyses of uranium oxide and steel samples have been made using a pulsed fast neutron activation analysis system. The uncertainty in the measured oxygen content of uranium oxide is ± 2.4%; that of steel varies from ± 13% at 30 ppm of oxygen to ± 4% at 300 ppm of oxygen. Samples were irradiated in a fast neutron flux of about 2×10^9 n cm^{-2} s^{-1} produced by 400 MeV deuterons on a tritium target. Sample N-16 γ-ray activities (produced via the $O^{16}(n,p)N^{16}$ reaction) were measured using a 35 cc Ge(Li) detector (for uranium) and a 3" x 3" NaI detector (for steel). Individual activities were normalised against the measured β-ray activity of N-16 produced in a conveniently located water sample. Relative oxygen concentrations were absolutely normalised against the N-16 γ-ray activity of standard samples. Extensive measurements and calculations were made to evaluate the relative importance of errors due to geometrical effects, electronic drift, γ-ray pile up and counting statistics. Ways in which the overall error can be significantly reduced are discussed.

1 – GENERAL CONSIDERATIONS SYSTEM DESCRIPTION

1.1 – INTRODUCTION

One of the principal uses of activation analysis with 14 MeV neutrons is the analisys of oxygen in different matrix structures[1,8,9,10,14]. Relative measurements are absolutely normalized against standard samples of known oxygen content. This work is concerned with the quantitative analysis of oxygen in both steel and uranium oxide fuel. Intense 14 MeV neutron sources are conveniently produced by the $T(d,n)^4He$ reaction using low voltage charged particle accelerators[6]. These neutrons react with oxygen to produce ^{16}N via the $^{16}O(n,p)$ ^{16}N reaction, having a threshold energy of 10,3 MeV and $\sigma(n,p) \cong 40$ mb. ^{16}N decays with a half life 7.15 s[2] via β-and- γ-ray emission (Figure 1). The short irradiation time to saturation for this reaction, coupled with the high energy of the emitted γ-rays (7.11 MeV and 6.13 MeV), significantly reduces the importance of most of the possible interfering reactions.

Direct interference is possible only by fluorine, via the $^{19}F(n,\alpha)^{16}N$ reaction, and boron, via the $^{11}B(n,\alpha)^8Li$ and $^{11}B(n,p)^{11}Be$ reactions. Fissile materials, if present, introduce a high background level.

Of these materials, only boron is present in significant quantities in special steels. Interfering effects due to the 13 MeV and 11.5 MeV β-rays of ^8Li and ^{11}Be may be eliminated by differential β-ray attenuation or significantly reduced by careful choice of the irradiation/counting cycle. Attenuation of the N-16 γ-rays by the former method can be important in very low oxygen content steels. Since the interfering reactions may be eliminated, quantitative analysis of oxygen in steel may be effected using a NaI(Tl) detector. Precise quantitative measurement of the oxygen in uranium oxide fuel by fast neutron activation analysis is complicated by the high fission product activity. The N-16 γ rays must be adequately resolved and should be detected with a high efficiency. Pre-amplifier saturation due to low energy fission product γ-rays must be eliminated and pile up eliminated or allowed for. In general the low integral count due the N-16 activity is the principal source of uncertainty in the analysis.

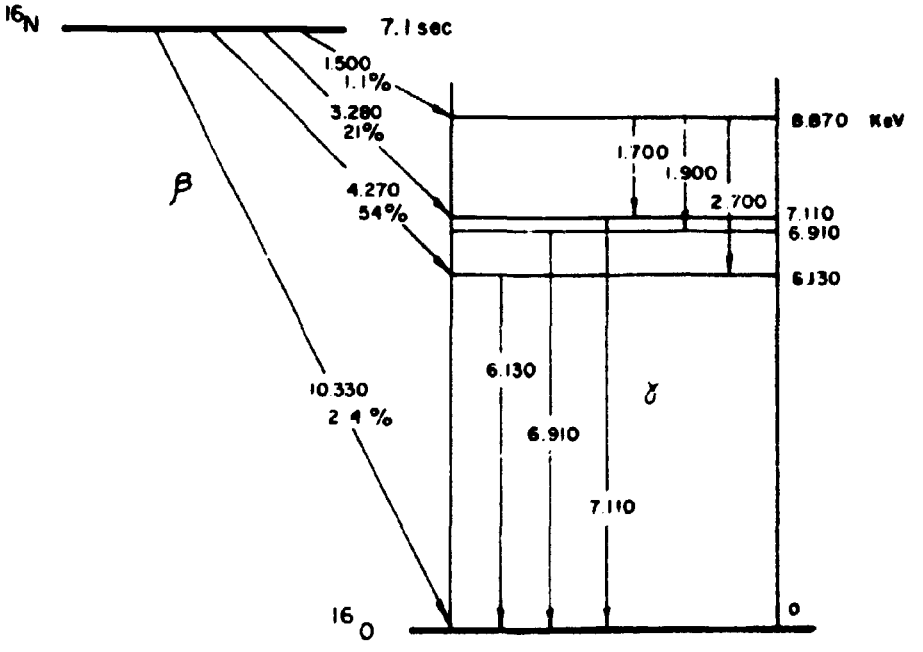

Figure 1 – Nitrogen-16 decay scheme

1.2 – EQUIPMENT

14 MeV neutrons were produced by the $T(d,n)^4He$ reaction using a 400 KV Van de Graaff accelerator with a conventional triated titanium target of effective diameter 22 mm. Square pulses of maximum intensity approximately 10^{10} n s^{-1} were produced by post acceleration mechanical interruption of the 150 μA deuteron beam. At the measured source to sample separation of 5 mm the neutron flux was of the order of 2×10^9 n cm^{-2} s^{-1}.

The source intensity was monitored using an NE-102 plastic scintillator to measure the N-16 β activity (E_{β^-} = 10.3 MeV) of a re-entrant surounding water cylinder of wall thickness 5 cm. Location of the test sample between the source and monitor resulted in attenuation of the fast flux at the monitor position. The scintillator was directly coupled to an RCA-6342A photomultiplier used with conventional electronics. During sample irradiation the photomultiplier high voltage was automatically switched off. By simultaneously irradiating and then counting both the monitor and test sample, the ratio of the monitor to sample counts is made independent of both neutron source fluctuations and the irradiation counting cycle[10].

Samples were pneumatically transferred between the irradiation and counting stations in aluminium tubing of internal rectangular cross section 9.5 mm x 22.3 mm. This ensured that the sample face closest to both the source and the detector was specified. Although transfer was typically between 0.5 to 1s using nitrogen gas at 20 to 40psi, a minimum wait time of 1.2s was necessary for the PM tube to restabilize. Activated samples were counted in a lead walled housing, of wall thickness 10cm and internally lined with copper sheeting located approximately 10m from the neutron source.

Separate counting configurations were used for the uranium and steel measurements (Figures 2 and 3). A schematic of the total experimental system is shown in Figure 4. Irradiation transfer and counting times were controlled with a Texas Nuclear 9615 Rapid Transfer Control Unit. Each counting irradiation cycle was separately and manually initiated. Production of neutrons by the $D(d,n)^3He$ reaction on the accelerator beam stop was prevented by manually reducing the accelerating voltage to zero immediately after irradiation. Prior to the start of the following irradiation the voltage was reset to 400 KV.

1.3 – THEORETICAL BASIS

The mass mo, of oxygen in the test sample is calculated using

$$mo = K_1 A/M \qquad (I)$$

where A and M are respectively the total counts due to the sample and monitor and K_1 is a constant for a given experimental configuration. A is given by

$$A = mo\, C_A\, E_A\, N_A\, \theta\, \sigma_A\, S_1\, S_2/M_o \qquad (II)$$

where the symbols have the following meanings.

C_A – constant which allows for neutron attenuation within the sample and self absorption of the emitted γ-rays by the sample.

E_A – intrinsic detector efficiency for N-16 γ-rays for the specified discriminator level.

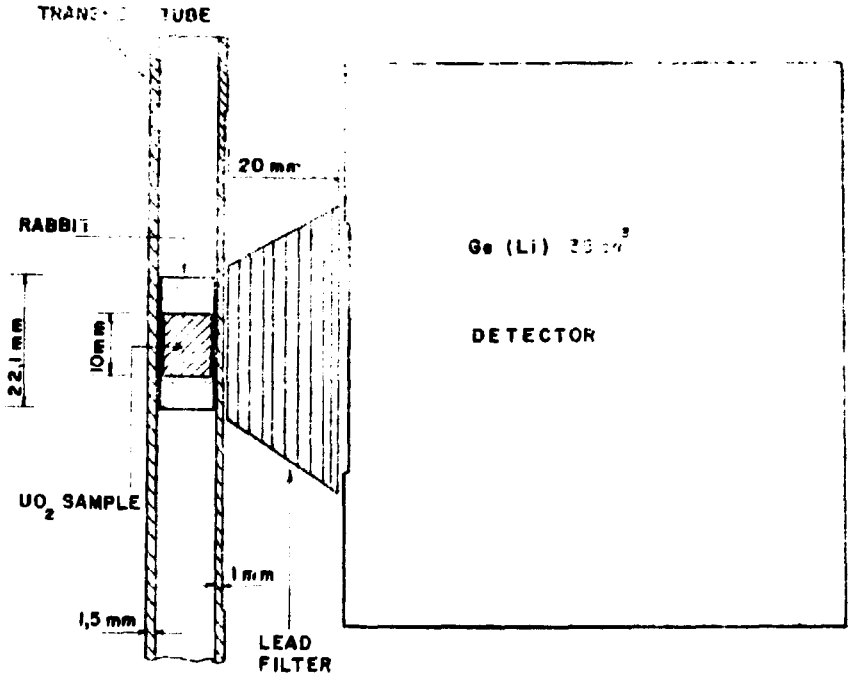

Figure 2 — Counting configuration for UO_2 sample measurements

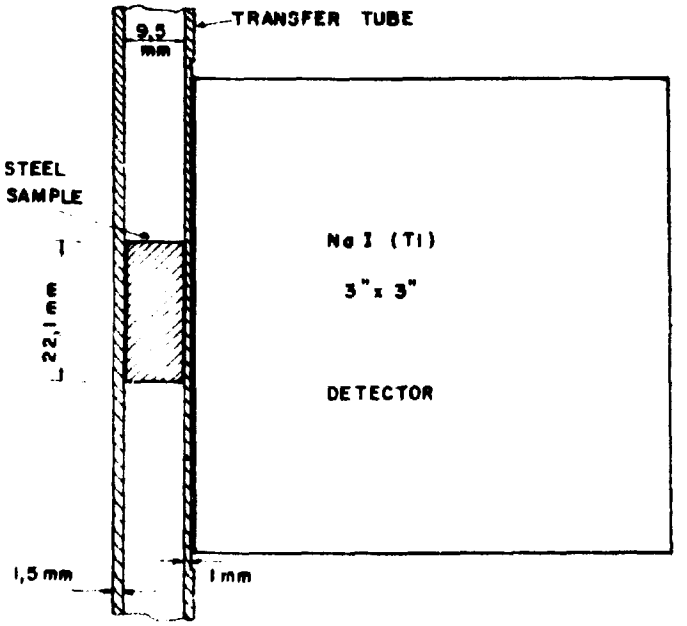

Figure 3 – Counting configuration for steel sample measurements

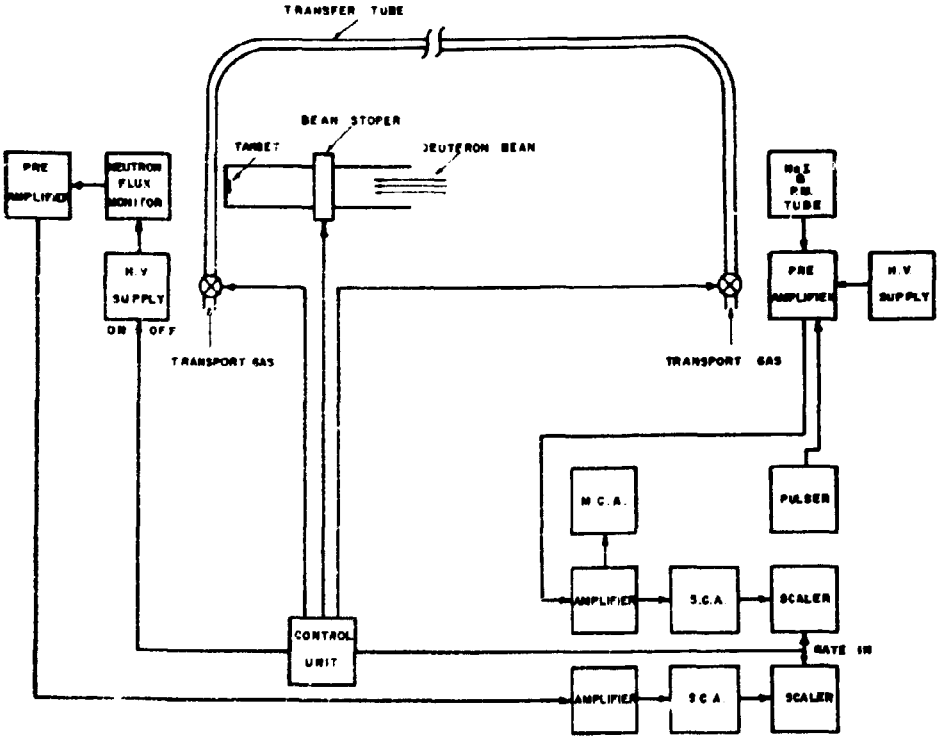

Figure 4 — Experimental system for analysis of oxygen in steel

N_A – avagadro's number

θ – isotopic abundance of ^{16}O

σ – cross section for the $^{16}O(n,p)^{16}N$ reaction for 14 MeV neutrons.

ϕ_A – mean fast neutron flux in the test sample.

S_1 – saturation irradiation factor = $1 - \exp(-\lambda t)$

S_2 – decay factor during sample counting = $\exp(-\lambda t_1) - \exp(-\lambda t_2)$.

M_o –atomic mass of oxygen.

The monitor count is given by

$$M = m_{oM}\, C_M\, E_M\, N_A\, \sigma\, \theta\, \phi_M\, S_1\, S_2\, \exp(-\Sigma d)/M_o \qquad \text{(III)}$$

where $\exp(-\Sigma d)$ is the attenuation of the neutron flux (at the monitor position) by the sample being irradiated and ϕ_M is the mean unattenuated 14 MeV neutron flux in the monitor. Equations (II) and (III) give

$$A/M = m_o\, C_A\, E_A \phi_A\, m_{oM}\, C_M\, \phi_M \exp(-\Sigma d) \qquad \text{(IV)}$$

and

$$K_1 = m_{oM}\, C_M\, E_M\, \phi_M\, \exp(-\Sigma d)/C_A\, E_A\, \phi_A \qquad \text{(V)}$$

Results are evaluated using a normalized count given by

$$C = Z\, A/M \qquad \text{(VI)}$$

Where Z is an arbitrary constant

Thus

$$m_o = KC \qquad \text{(VII)}$$

where

$$K = K_1\, A$$

The oxygen to uranium ratio, R, is related to the normalized count through the relationship

$$R = \frac{M_U/M_O}{M - KC}\, KC \qquad \text{(VIII)}$$

where

M_U = atomic mass of uranium

M_O = atomic mass of oxygen

M = sample mass.

1.4 – SOURCES OF ERROR

In equation V., above K will be constant provided that electronic drift is negligible, the irradiation and counting geometries are fixed and the samples are dimensionally equal and of essentially similar compositions and density. The principal sources of error introduced by assuming K is constant are due to system gain and discriminator level changes and irradiation drift. These are corrected for by periodically normalizing against a standard sample of high oxygen content. For small source to sample separations, slight changes in the effective source position result in large sample activity changes. (Figure 5). By defocussing the accelerator beam this effect is reduced. (Figure 6). Reduction of the target current to 80% of the beam current by defocussing reduced errors additional to counting statistics to approximately 1,5%. For small source to sample separations sample inhomogeneity can introduce a further source of error due to the high $1/r^2$ flux gradient close to the source. The magnitude of this effect can be evaluated by measuring the change in count rate when the sample orientation with respect to the source is reversed.

1.5 – SYSTEM TESTS

Effects due to interfering reactions in the monitor counts can be largely eliminated by correct adjustment of the discriminator level. The correct setting was taken to be that which gave the known N-16 decay constant evaluated by least squares fitting the time decreasing activity to an exponential plus constant background. To within statistics this decay constant was unchanged when data obtained in the first three half lives was discounted. For this discriminator level the ratio of the N-16 counts to background counts was less than 0,5%. These measurements additionally showed that the photomultiplier was stabilized approximately 1.2s after its high voltage supply was switched on.

Measurements were made to evaluate the magnitude of errors due to source intensity variations. The influence of geometrical effects was largely eliminated by irradiating a cylindrical homogeneous Lucite sample, (33% oxygen), of diameter 22 10 mm and thickness 9 4 mm, at a source to sample separation of 62 mm and subsequently counting at a sample to detector separation of 60 mm. The normalized sample count was essentially unchanged for fixed source outputs of between 0,5 max. and max. intensity (Table I). In an additional measurement for which the detector to sample separation was reduced to the standard value of 1 cm the total error was reduced to 1.3% with a counting error of 1.2% These two sets of measurements therefore showed that the non statistical (counting) error of 1.5% obtained for standard conditions was predominantly due to geometrical effects at the irradiation terminal.

2 -- URANIUM OXIDE MEASUREMENT

2.1 – INTRODUCTION

Most power reactors now in operation, or which are planned to be in operation before 1982, use ceramic uranium dioxide fuel in the form of pellets. Absorption of oxygen in excess of the stoichiometric formula UO_2 leads to higher oxide production and an oxygen to uranium ratio (U/O) greater than 2. Because many properties of ceramic fuel, such as thermal conductivity, fusion point, etc, are significantly effected by this ratio[7,11,16,23], it must be held to between 2 00 and 2.02 (ASTM-C696-72). Fuel pellets

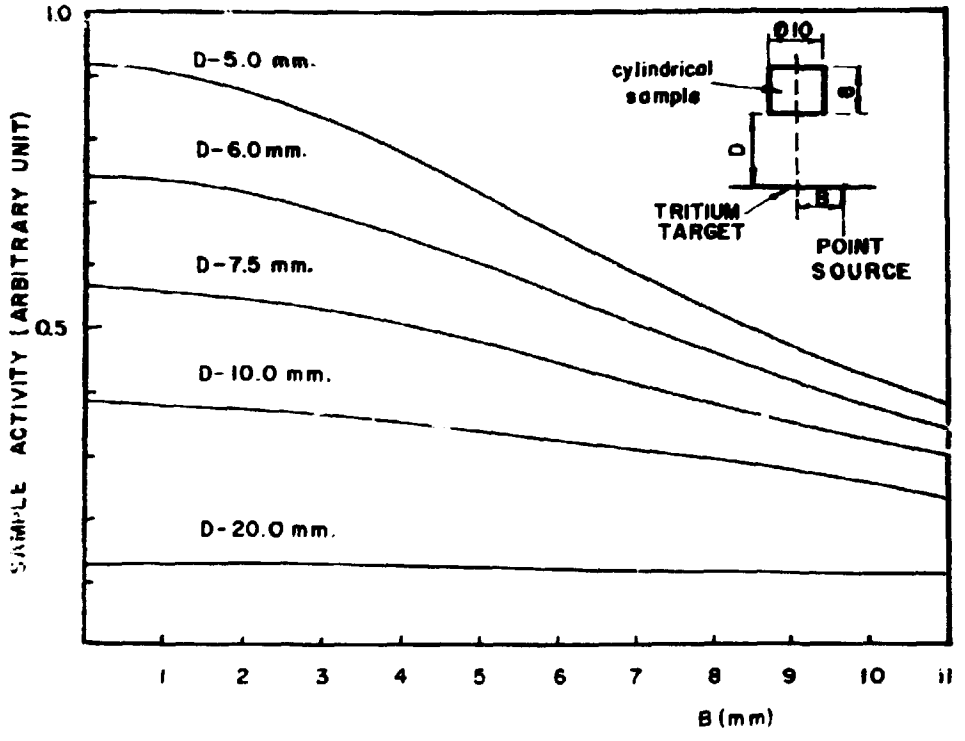

Figure 5 – Calculated change in sample activity with the off–axis target separation (B) – The curves were calculated using numerical integration of the flux over the sample volume; $1/r^2$ flux attenuation was assumed

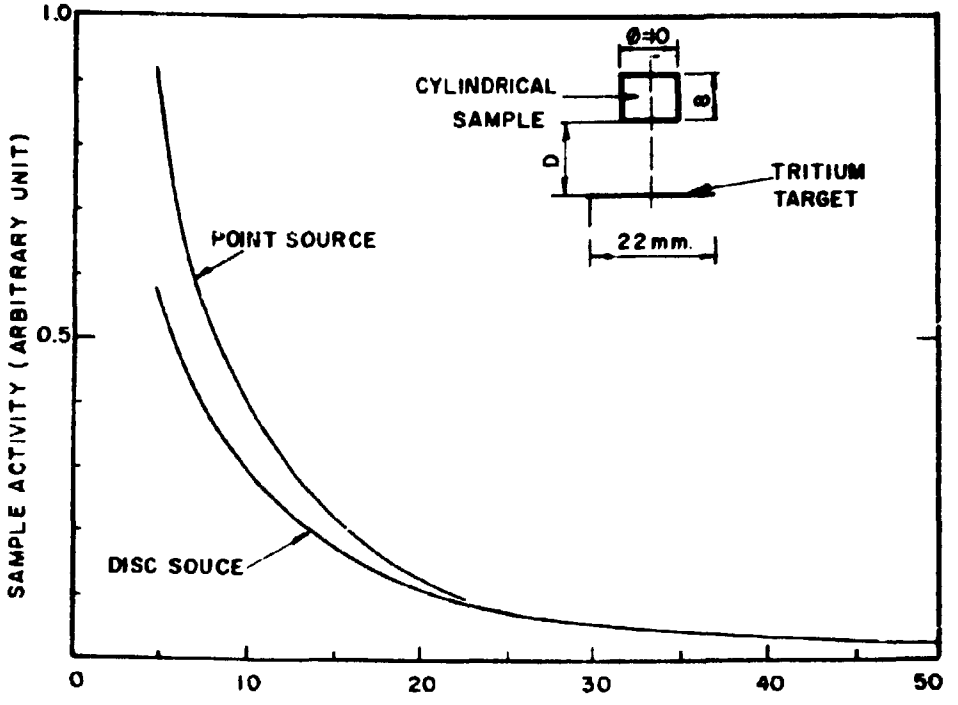

Figure 6 — Calculated change in sample activity with the sample to target distance (D).
— The curves were calculated as indicated in figure 5

are fabricated by sintering pellets of compressed UO_2 powder The shrinkage during sintering, and hence the final pellet density, is significantly dependent on the initial O/U ratio

Table I

Irradiation of Lucite sample with different neutron yields. $\bar{\sigma}_{exp}$ is the mean of the expected standard deviation considering only counting statistics

Neutron yield [% of max.]	Number of determinations	Normalized counts average [C]	Expected mean standard deviation $[\bar{\sigma}_{exp}]$	Observed standard deviation $[\sigma_{obs}]$
100	25	1136	35.6	28.0
80	25	1123	39.5	35.5
50	16	1131	49.4	43.2

To date the methods must frequently used to measure this ratio utilise the weight change during oxidation to U_3O_8[23], the measured ratio of U (VI) and U (IV)[5] or the direct measurement of the excess oxygen by reduction in a CO atmosphere[5,22]. Although sufficiently precise, these methods are both destructive and slow

Details of quantitative measurements by fast neutron activation analysis, typically requiring less than 1 hour per analysis, are here given Modifications to the experimental system are proposed which should reduce the measured uncertainty of ± 2.8%, high because of poor counting statistics, to significantly less than 1%.

2.2 – EQUIPMENT

Details of the activation analysis system have already been given in section 1 2 Sample activities were measured with a 35 cm^3 Ge(Li) detector. The sample and detector were separated by a 2 cm lead filter (Figure 2) to attenuate the low energy γ-rays emitted by the fission products in the sample A thinner filter resulted in the preamplifier charging rate of 45 000 MeV s^{-1} being exceeded at the start of the counting cycle Figure 7 shows a schematic of the counting electronics, in which the 444 ORTEC biased amplifier has base line restore and automatic pile up rejection Because of the initial very high activity of short lived fission products, both the system gain and resolution vary with activity decay Pulse height spectra in a given counting cycle were therefore successively stored in the 4 memory stores of the 1024 MCA using a specially constructed switching circuit

2.3 – MEASUREMENTS AND EXPERIMENTAL RESULTS

Measurements were made using compacted UO_2 samples of 10 mm diameter, 8 mm thick and weight approximately 3 2 gms. This was necessary because sinterred uranium oxide samples with a wide spread of O/U ratios were not available Samples were precisely located in thin walled aluminium rabbits of low oxygen content Irradiation, wait and count times of 15,2 and 30 seconds were used The counting time was subdivided into three 5 second intervals and one 15 second interval Each analysis was made using the integral counts collected over 16 irradiation/counting cycles For a given analysis the average count due to the rabbit and rabbit plus sample was 2,5 and 2000 A schematic of the sample counting electronics is given in Figure 7

Spectra were read out on perforeted tape and the integral counts due to N 16 (6 13 MeV plus 1st

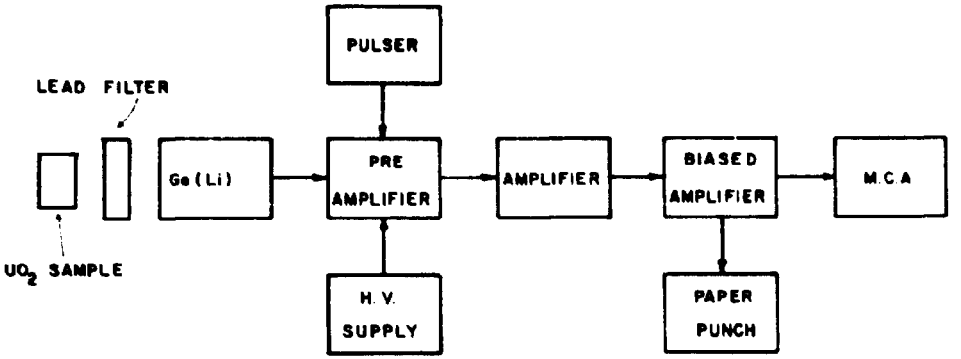

Figure 7 – Schematic of the electronics used for sample counting in o/u measurements

2nd escape peaks) was calculated by least squares fitting the data to a Gaussian plus linear background. Representative spectra are shown in figures 8 and 9. Calculations were made using the BASIC program AREAN-16 run on a 16 K memory Hewlett Packard 2116 C computer.

Results of analysis of sample 1 data are given in table II; table III summarises the results of 6 additional analyses and includes results of chemical analysis. Figure 10 shows the calibration curve for the system, calculated by least squares fitting the data in Table III to equation (VII). The proportionality constant K, calculated using the data in table III, is $(2.23 \pm 0.01) \times 10^{-4}$ g count^{-1}.

2.4 – CONCLUSIONS AND SUGGESTIONS

With the equipment used the mean square deviation of the integral normalised counts obtained in 16 sucessive irradiation/counting cycles was 2.5%; this is close to the value of ± 2.4% due to counting statistics alone

This precision is adequate for unsinterred UO_2 powder but is inadequate for ceramic fuel rods to be used in power reactors. For the latter the oxygen/uranium ratio must be within the range 2 to 2.02 (ASTM-C696-72).

Several ways in which the uncertainty in the measurements may be reduced are as follows:

– increase the maximum possible count rate of the pre-amplifier by reducing the feedback resister. For an acceptable loss in resolution, of the order of 3KeV, a five fold increase in count rate is possible*.

– Increase the sample size

– Increase the number of irradiation/counting cycles per analyzed sample.

– Use a higher efficiency detector. The 35 cc Ge(Li) detector used has an efficiency of 5% compared to a 3" x 3" NaI(Tℓ) detector, for the 1.33 MeV Co^{60} γ-rays. Single detectors of efficiency 18% and double detector systems of overall detection efficiency 30% are commercially available. With these the 7.11 MeV γ-rays from N 16 (21% of the decays) can also be measured.

– Increase the source intensity of 10^{10} ns^{-1}. Generators of intensity approximately 10^{12} ns^{-1} are commercially available[13]

– Use special techniques to both reduce and correct for γ-rays pile up.

A particularly powerful technique to correct for γ-ray pile up, base line shift and dead time losses is to introduce pulses of fixed amplitude, close to the γ-ray peak of interest, into the preamplifier test input. The pulse repetition frequency is reduced at approximately the same rate as the decay of the measured activity. The total loss of counts under the specified peak is then calculated from the ratio (integral number of pulses)/(measured counts) for the pulser peak. Overall uncertainties (errors) inclusive of counting statistics, of ± 0.2% have been reported for experiments in which 60 % loss in peak counts occurs.[3]

– Modification of the irradiation terminal

---

* Discussion with ORTEC technical representative

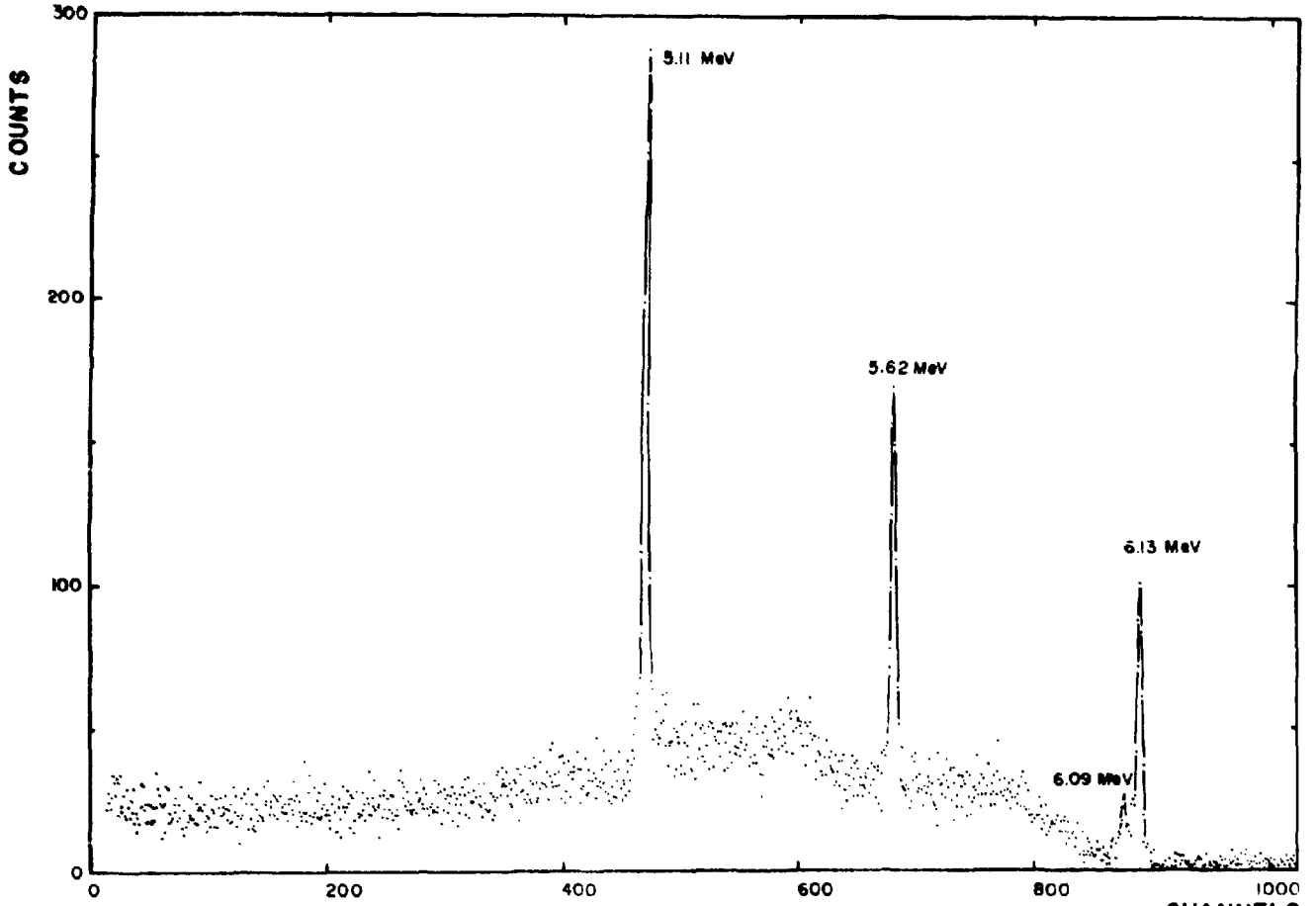

Figure 8 — Spectrum of N 16 in Lucite sample obtained with Ge(Li) detector

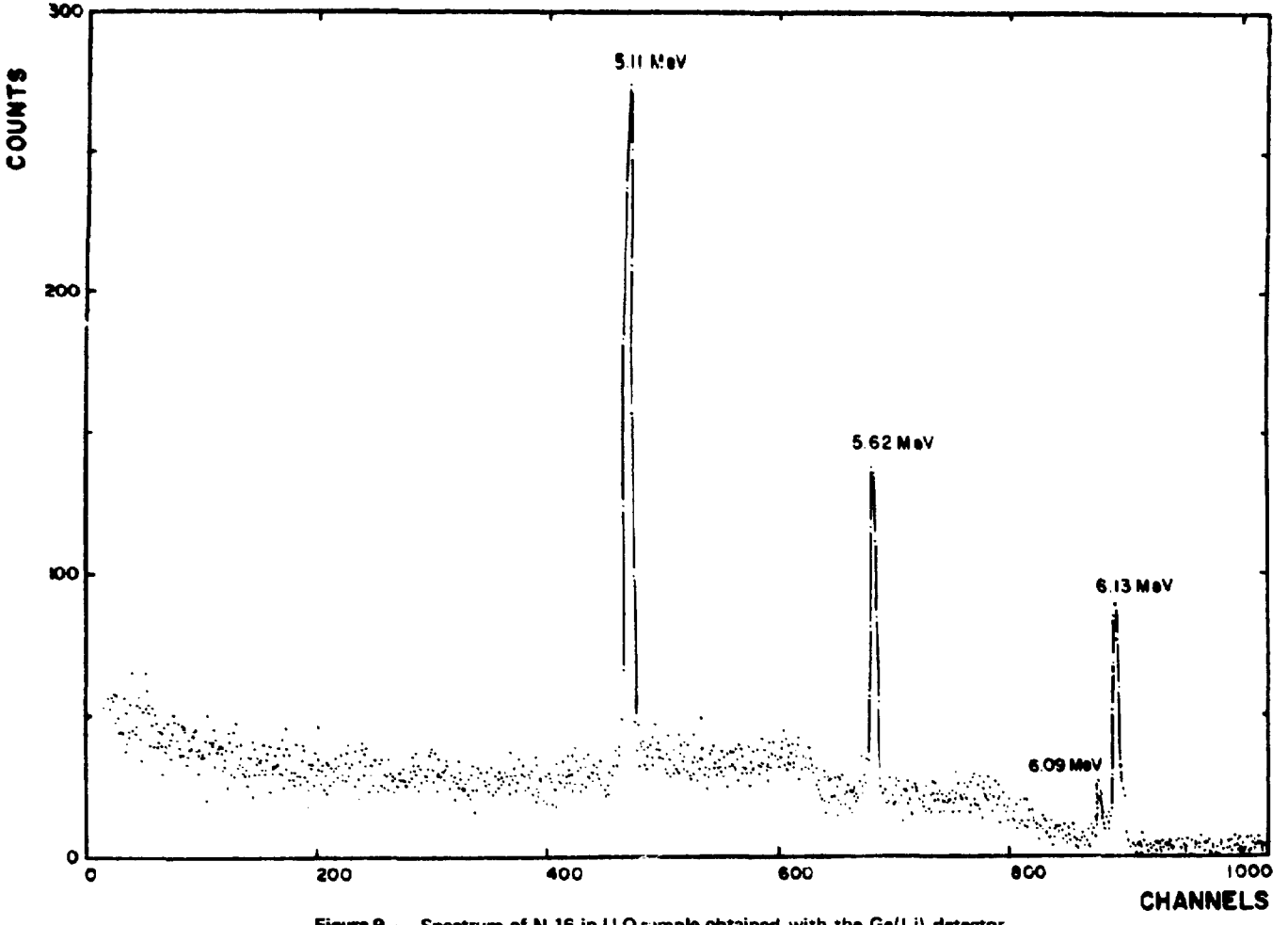

Figure 9 — Spectrum of N-16 in U O sample obtained with the Ge(Li) detector

Table II

Counts obtained in the irradiations of sample number 1

Determination number	Number of irradiation	Monitor counts M	SAMPLE COUNTS					Normalized counts ($=2.5 \times 10^5 . \frac{A}{M}$)
			1^{st}spectrum A_1	2^{nd}spectrum A_2	3^{rd}spectrum A_3	4^{th}spectrum A_4	Total A	
1	16	239319	799.6	533.3	319.7	367.8	2020	1745
2	16	296280	775.8	527.6	348.3	378.8	2031	1713
3	16	278643	683.0	493.7	301.6	391.3	1870	1679
4	12	213956	609.0	354.2	204.6	288.2	1456	1701

Table III

Counting Data for Irradiated UO_2 Cylindrical Samples

Sample number	Weight (g)	O/U ratio chemical method (R)	Number of determinations	Normalized counts (C)	Expected standard deviation (σ_{exp})	Observed standard deviation (σ_{obs})	Normalized counts average ($\bar{C}$)
1	3.272	2.033	4	1745 1713 1679 1701	38.5 38.1 39.3 44.8	27.8	1710
2	3.291	2.031	5	1704 1658 1701 1627 1722	35.9 37.1 39.9 39.9 40.8	38.9	1682
3	3.249	2.113	4	1728 1776 1824 1830	45.1 42.5 43.5 45.3	48.0	1790
4	3.211	2.098	4	1700 1790 1783 1741	45.2 42.6 42.1 42.7	41.5	1754
5	3.285	2.029	4	1760 1769 1679 1683	41.0 42.4 42.3 42.8	48.3	1723
6	3.268	2.122	3	1846 1742 1770	44.2 44.6 45.4	53.4	1786

Imprecise sample position and effective source movement on the accelerator target may significantly increase the overall uncertainty in the measurements. When data blocks of 16 measurements are summed the single measurement non-counting error of ± 1.5% is reduced to ± 0.37%. By rotating both the sample and monitor in the fast neutron flux, geometrical errors may be essentually eliminated[17,19].

In summary, measurement of the oxygen/uranium ratio by fast neutron activation analysis was shown to be sufficiently accurate for the analysis of uranium oxide powder prior to sinterring. Implementation of the itemised modifications should result in an overal uncertaintly in this ratio of significantly less than 1%. Fast neutron activation analysis, both non destructive and relatively rapid, would then be sufficiently precise for measurement of the O/U ratio of ceramic uranium oxide fuel pins to be used in power reactors.

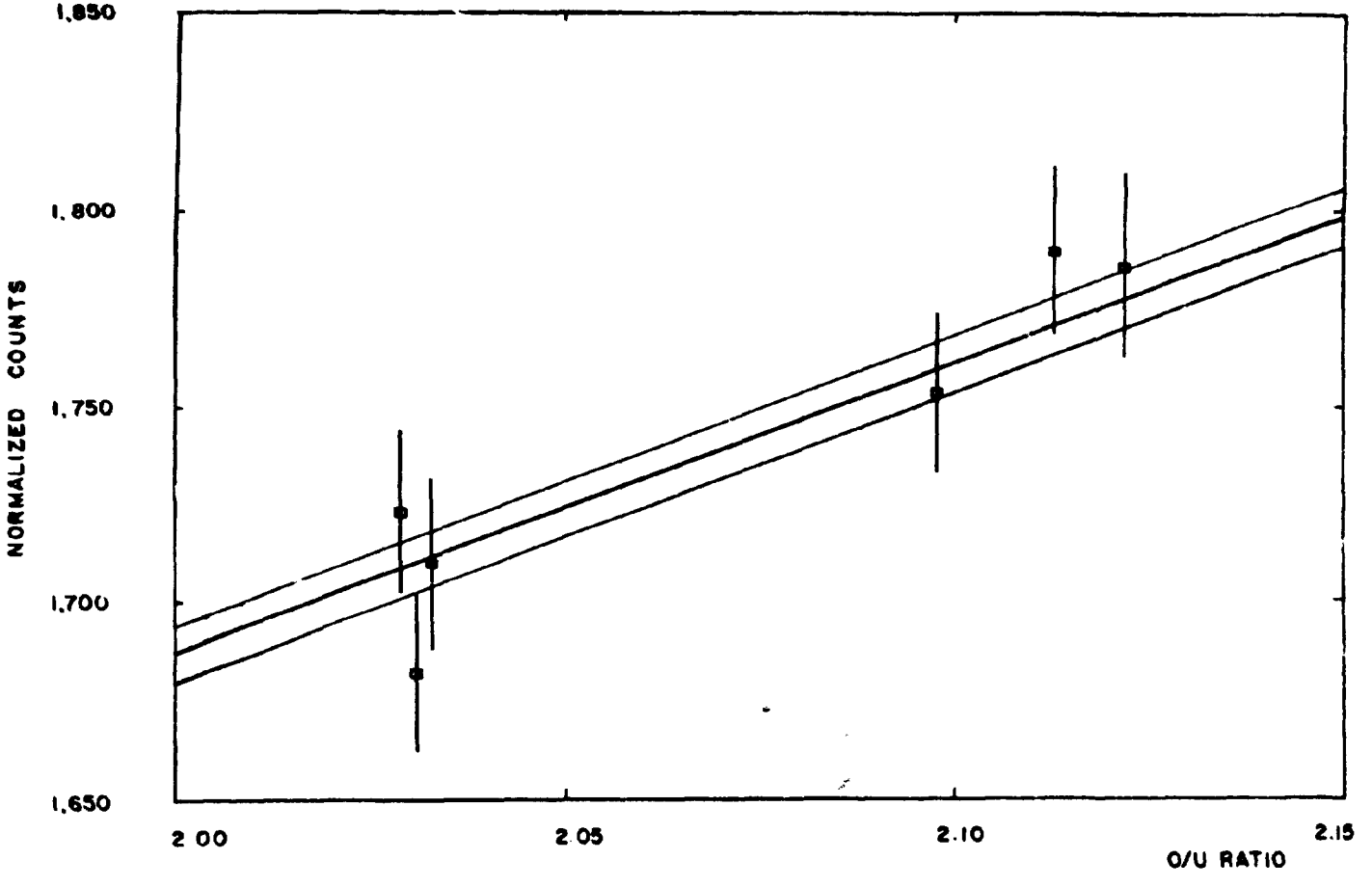

Figure 10 — Calibration curve for the determination of the o/u ratio in test samples

3 – OXYGEN IN STEEL

3.1 – INTRODUCTION

In the manufacture of special purpose steels it is necessary to control and therefore measure the oxygen content[20,21], typically specified to be within a range measured in parts per million (ppm). Viable methods of measuring the oxygen in steels during commercial production are fusion reduction under vacuum or an inert gas, measurement of the electromotive potential of the fused steel "bath" and 14 MeV neutron activation analysis[4]. The first is precise but suitable only for small samples ($\leq$ 0.5 gm). Interpretation of results obtained by the second method is dependent on operator judgement[6] and, additionally, analysis of solidified steel is not possible.

Quantitative oxygen analysis of steels by 14 MeV neutron activation analysis is a proven non-destructive technique in which samples of up to 30 gms may be analysed.

This work was undertaken to test the suitability of an experimental fast neutron activation analysis system of steel in steel manufacture.

3.2 – EQUIPMENT DETAILS AND SETTINGS

The experimental system has been earlier described and is shown in schematic form in figures 3 and 4. Irradiation, wait and counting times of 15 s, 2 s and 30 s were used. For this irradiation the N-16 activity was approximately 77% of the satured activity and production of the interfering isotope Mn-56 (T1/2 = 2.6 h; E(γ) between 0.84 and 3,2 MeV) was minimal. At the completion of the counting period the N-16 activity was reduced to 5.4% of its initial value. A 3" x 3" NaI(Tl) detector separated 3 mm from the sample was used. The single channel analyzer was used in the integral mode with a descriminator cut off equivalent to a γ-energy of 4.6 MeV. Pulses above this level were essentially due to N-16 activity. As earlier stated the sample and monitor were simultaneously counted.

3.3 – SYSTEM TESTS

A series of measurement was made to check the reproducibility of measurements and to estimate the experimental errors of the system for the specified irradiation/counting cycle. Results of these measurements in which a high oxygen containing sample was used are summarized in Table IV below.

Table IV

Results of Reproducibility Measurements

C	σ^2_{obs}	σ^2_{exp}	σ_{obs}	σ_{sys}	n
3763 ± 13	10269	7024	101 (2,69%)	56.8 (1,51%)	60

were:

$\overline{C}$ – mean of normalized counts

σ^2_{exp} – expected variance calculated assuming only counting errors.

σ^2_{obs} – observed variance in the measurement $\dfrac{\Sigma(C - \bar{C})^2}{n-1}$

σ_{sys} – system experimental standard deviation

$$\sigma_{sys} = \sqrt{\sigma^2_{obs} - \sigma^2_{exp}}$$

n – number of irradiations

3.4 – SYSTEM CALIBRATION

The relative quantity of oxygen in a test sample is given by

$$m_o = K_1 \frac{A}{M} \qquad (1)$$

where the terms have been previously defined. K_1 is evaluated from the counts due to a standard sample of known oxygen content. The error in K_1 will be reduced by using several standards of different oxygen content and applying a least squares fit to the count data.

Five standard irradiation samples 9.4 mm high and 6.35 mm diam. were cut from NBS standards of the same diameter. Other homogeneous 'standards' of diameter 22.1 mm were cut from steel bars of standard diameter 22.1 mm. Two discs of thickness 9.4 mm were cut from each bar and the diameter of one disc of each pair was reduced to 6.35 mm to anable a direct intercalibration with the NBS standards to be made.

3.5 – SAMPLE CALIBRATION AND STABILITY CHECKS

A special rabbit was made from steel of very low oxygen content to transfer the 6.35 mm diameter samples between the irradiation and counting station. Results of the measurements made on the NBS standards are summarized in table 5. A least squares fit to the data was made using the BASIC code GENFIT in which errors in two dimensions are allowed. The calibration curve so obtained is given in figure 11. Results for the two sets of "sub-standards" are summarized in table 6. The oxygen content of the smaller disc was directly calculated using the calibration constant K_1 evaluated from the NBS data. The calibration graph for the 'sub-standards' is given in figure 12.

Irradiation tests; made before reducing the disc diameter from 22.1 mm to 6.35 mm, showed that the oxygen concentration of each of a given pair of discs were equal to within 1%.

The importance of possible instabilities in the counting electronics was checked by measuring (mean of 4 irradiations) a high oxygen content sample after every 40 sample irradiations.

Table V

Experimental results for NBS standards

NBS SAMPLE	1090	1091	1093	1092	1094	RABBIT
PPM of 0	490 ± 10	130 ± 4	60 ± 5	28 ± 2	45 ± 2.5	0
Mean counts (7 measurements)	210 ± 5.4	80.4 ± 3.3	62.4 ± 3	42.6 ± 2.4	37.7 ± 2.3	30.8 ± 2.4
Variance	191	33	63	33.3	37	22.3
Expected Variance	206	74	61	40.5	36	27.8

Note: The oxygen content of the 'rabbit' was equated to zero for calculational purposes. Oxygen in the rabbit will effectively increase the background level.

Table VI

Experimental results for secondary standards

Sample	2	3	VT–20	6	NBS 734
Sample Diameter = 6.3 mm (7 measurements per sample)					
Mean counts	76 ± 3.4	61.4 ± 2.8	64.8 ± 2.9	137.6 ± 4.6	63.4 ± 3.7
Variance	80	32	45.7	148.3	93.5
Expected Variance	72	54.3	60.2	134.2	68.6
PPM of 0	116 ± 9.5	75.8 ± 7.8	85.1 ± 8.5	285.7 ± 13.5	81.3 ± 10.2
Sample diameter = 22.1 mm (10 measurements per sample)					
Mean counts	251 ± 7	156 ± 5.7	177 ± 5.9	620 ± 9.5	192 ± 6.5
PPM of 0	116 ± 9.5	75.8 ± 7.8	85.1 ± 8.5	287 ± 13.5	81.3 ± 10.2

OBS: The quoted error on the oxygen content is calculated using

$$\sigma = [\ \sigma DM^2 + \sigma CAL^2\ ]^{1/2}$$

Where σ_{MD} = standard deviation on the sample counts, in ppm of oxygen;

σ_{CAL} = error due to the least squares data fitting of the NBS standards (ppm of 0).

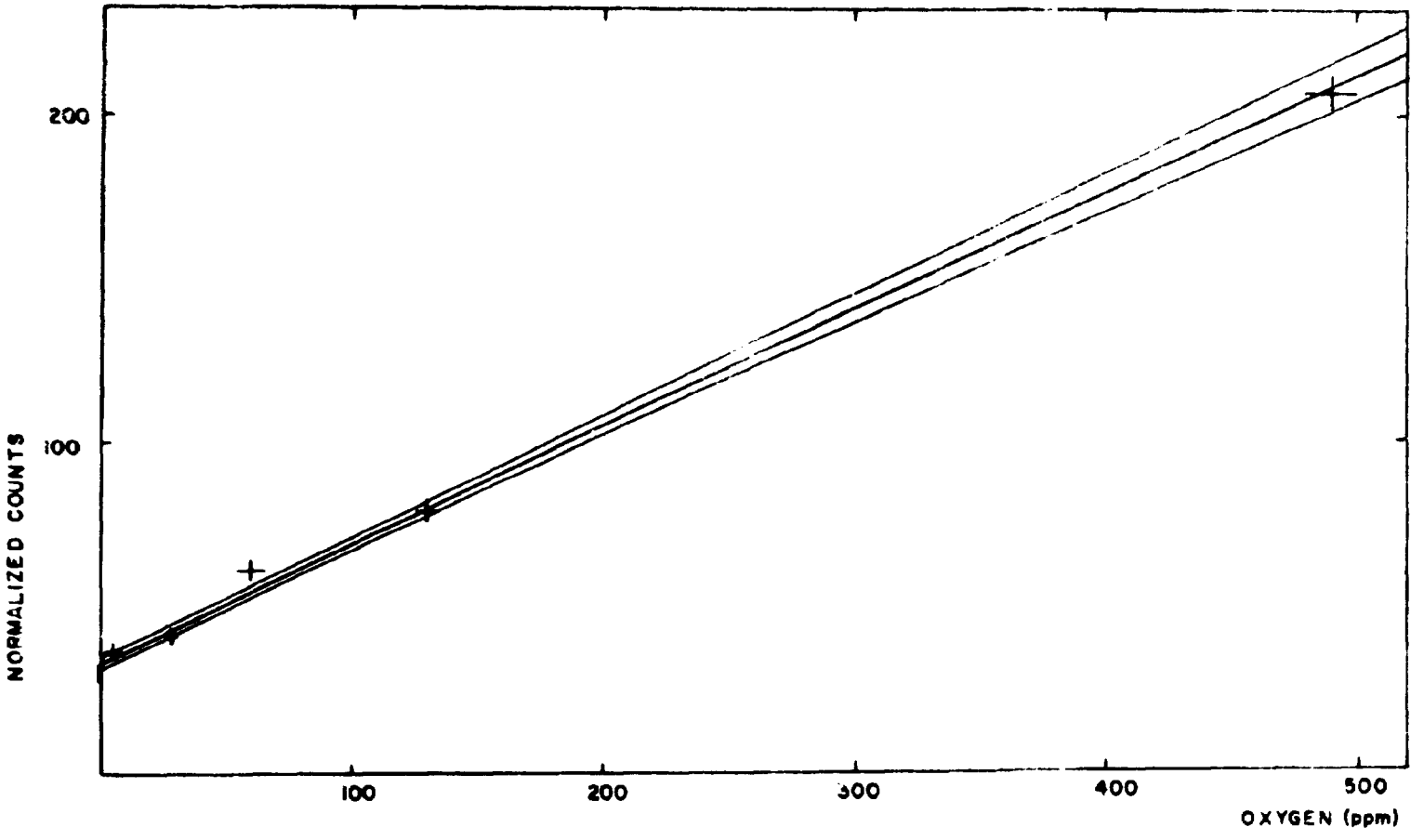

Figure 11 — Calibration curve for the determination of oxygen in steel (Sample Diameter: = 6.35 mm).

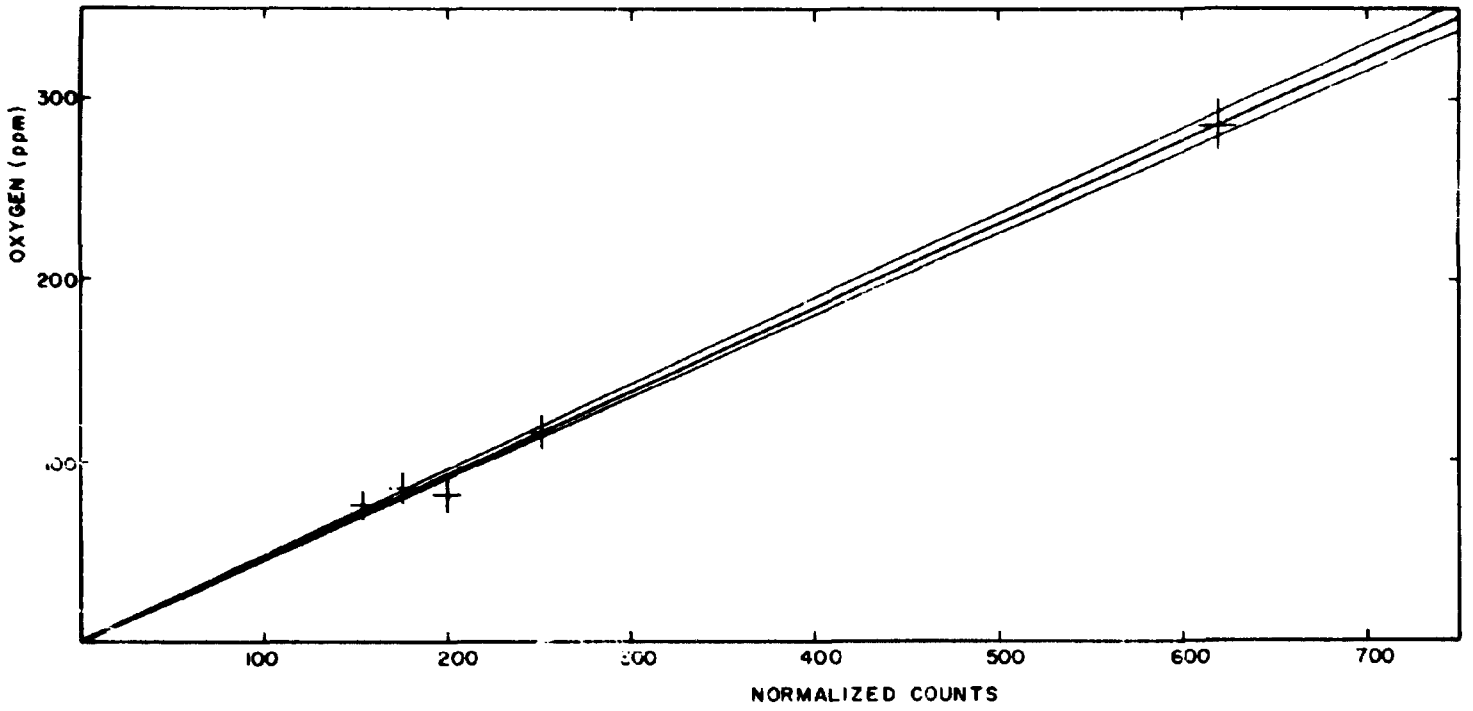

Figure 12 — Calibration curve for the determination of oxygen in steel (sample diameter: ϕ = 22.1 mm).

When consecutive "check" measurements differed by less than 0,5% no correction was made. The maximum correction after 200 measurements taken on the same day was less than 3%.

3.6 – RESULTS OF MEASUREMENTS

Measurements were made on 20 steel samples of standards dimensions with oxygen contents in the range 30 to 370 ppm. The mean and RMS error for each sample was calculated from 10 measurements. Typical error values for the different oxygen containing steels are as follows; 30 ppm – 13%, 70 ppm – 9%, 120 ppm – 6%, 300 ppm – 4%. Additional measurements, each of 10 irradiations, were made on three different days to check long term reproducibility. A maximum change of ± 4% was observed but more usually results were reproducible to better than ± 1%.

3.7 – CONCLUSIONS

Results of quantitative oxygen analysis in steel using a fast neutron activation analysis system have been presented. These measurements are adequately precise for the control of oxygen concentrations in the fabrication of both normal and special purpose steels. By linear extrapolation to higher efficiency detection systems, replacement of the single 3" x 3" NaI(Tℓ) detector by two 3" x 3" detectors or two 5" x 5" detectors would respectively reduce the lower detection limit from 3 ppm to 1.7 ppm and 0.9 ppm. For the lower oxygen value the standard deviation on a single measurement would be of the order of ± 50%.

RESUMO

Foram executadas análises quantitativas do oxigênio em amostras de óxido de urânio e aço utilizando-se um sistema de análise por neutrons rápidos pulsados. A incerteza na quantidade medida de oxigênio foi de ± 2.4% para o óxido de urânio; de ± 13% para 30 ppm e ± 4% para 300 ppm de oxigênio nos aços. As amostras foram irradiadas em fluxos de neutrons rápidos de cerca de 2×10^9 n cm^{-2} seg^{-1} produzidos por dêuterons de 400 KeV incidentes sobre um alvo de trítio. As atividades gama do N-16 produzido via reação $O^{16}(n,p)N^{16}$ foram medidas utilizando-se um detector Ge(Li) de 35 cm^3 (para urânio) e um detector NaI de 3" x 3" (para os aços). As atividades individuais foram normalizadas com a atividade beta do N-16 produzido e colocado em local apropriado. As concentrações relativas do oxigênio foram normalizadas, de maneira absoluta, com a atividade gama do N 16 em amostras padrões. Medidas extensivas e cálculos foram feitos para avaliar a importância relativa dos erros provenientes dos efeitos geométricos, das flutuações eletrônicas, da justaposição de raios gama e da estatística de contagem. São discutidos também os meios para se reduzir significativamente os erros.

RÉSUMÉ

Des analyses quantitatives d'oxygène a partir d'echantillons d'acier et d'oxyde d'uranium ont été faites utilisant un system d'analyse d'activation par neutrons rapides pulsés. L'incertitude quand au contenu d'oxygéne mesuré de l'oxyde d'uranium est ± 2.4%; celui de l'acier varie de ± 13% à 30 ppm d'oxygéne à ± 4% a 300 ppm d oxygene.

Des échantillons ont été irradiés dans un flux de neutrons rapides d'approximativement 2×10^9 n.cm^{-2}.s^{-1} produit par des deutérons de 400 KeV sure une cible de tritium.

Des activités du rayonnement γ d'un échantillon N-16 (produites via la réaction $O^{16}(n,p)N^{16}$) ont été mesurées utilisant un détecteur 35 cc Ge(Li) pour l'uranium et un détecteur au NaI (3" x 3") pour l'acier.

Des activités individuelles furent normalisées par la mesure de l activité du rayonnement β du N-16 produit dans un échantillon d'eau.

Les concentrations relatives d'oxygéne furent normalisees de manière absolue par l'utilisation de l'activité du rayonnement γ (N-16) d'échantillons standards.

Des mesures extensives ainsi que des calculs ont ete faits afin d'évaluer l'importance relative des erreurs dues à des effets géometriques, dérive electronique, accumulation de rayonnement γ et statistiques de comtage. Les differents maniéres avec lesquelles l'erreur globale peut être significativement réduite sont également discutés.

REFERÊNCIAS BIBLIOGRÁFICAS

1. ANDERS, O. U. & BRIDEN, D. W. A rapid, nondestructive method of precision oxygen analysis by neutron activation. *Analyt. Chem.*, Easton, Pa., 36:287-92, 1964.

2. BIENLEIN, J. K. & KALSCH, E. The half-life of N^{16}. *Nucl. Phys.*, Amsterdam, 50:202-8, 1964.

3. BOLOTIN, H. H. et alii. Simple technique for precise determinations of countings losses in nuclear pulse processing systems. *Nucl. Instrum. Meth.*, Amsterdam, 83:1-12, 1970.

4. BRUCH, J. Determination of gases in steel and application of the results. *J. Iron Steel Inst.*, London, 210:153-62, 1972.

5. BURD, R. M. & GOWARD, G. M. *The polarographic determination of hexavalent uranium in uranium oxides: the determination of oxygen uranium ratios.* Pittsburgh, Pa., Westinghouse Electrical Corp., Bettis Atomic Power Division, Apr. 1959. (WAPD-205).

6. CATOUL, P. et alii. Control of the oxygen content of molten steel with the "Celox" cell. *C.R.M. metall. Rep.*, Liège (35):33-40, 1973.

7. CHRISTENSEN, J. A. *Stoichiometry effects in oxide nuclear fuels, I. Power rating required for melting and oxygen redistribution in molten center UO_{2} sub+-x. . .* Richland, Wash., Pacific Northwest Lab., Dec. 1967. (BNWL-536).

8. FUJII, I. et alii. Industrial activation analysis unit with 14-MeV neutron generator and its applications. *Toshiba Rev., Intern. Ed.* Tokyo (35):32-9, 1963.

9. GIJBELS, R. et alii. An oxygen standard for the determination of oxygen in steel by 14-MeV neutron activation analysis. *Analytica Chim. Acta.* New York, 43:183-98, 1968.

10. GILMORE, J. T. & HULL, D. E. Neutron flux monitoring for activation analysis of oxygen. *Analyt. Chem.* Easton Pa., 35:1623-5, 1963.

11. GODFREY, T. G. et alii. *Thermal conductivity of uranium dioxide and Armco iron by an improved radial heat flow technique.* Oak Ridge, Oak Ridge National Lab., June 1964. (ORNL-3556).

12. GORNER, W. An adaptation of the pulser method for the determination of losses in counting short-lived nuclides. *Nucl. Instrum. Meth.*, Amsterdam, 120:263-4, 1974.

13. HOLAND, L. & HAWKESWORTH, M. R. Low voltage particle accelerators for neutron generation. *Non-destruct. Test.*, Evanston, 4:330-7, 1971.

14. HOSTE, J. et alii. *The determination of oxygen in metals by 14MeV neutron activation analysis,* Belgium, University of Ghent, 1967, (EUR-3565e).

15. JONES, I. G. *The determination of oxygen metal ratios in uranium and uranium-plutonium dioxides.* Harwell, Berks., Atomic Energy Research Establishment, Process Technology Div., Jul. 1973. (AERE-R-6962).

16. KELLER, D. L. *Progress on development of fuels and technology for advanced reactors during January-March 1971: quarterly report.* Columbus, Ohio, Battele Memorial Inst., Apr. 1971. (BMI-1905).

17. LUNDGREN, F. A. & NARGOLWALLA, S. S. Use of a dual sample biaxial rotating assembly with a pneumatic tube transfer system for a high precision 14-MeV neutron activation analysis. Analyt.

Chem., Easton, Pa., 40:672-7, 1968.

18. MARCHANDISE, H. *Thermal conductivity of uranium dioxide: review report.* Luxemburg, Comm. of the European Communities, Nov. 1970. (EUR-4568).

19. MOTT, W. E. & ORANGE, J. M. Precision activation analysis with 14-million electron volt neutrons. *Analyt. Chem.*, Easton, Pa., 37:1338-45, 1965.

20. MUNDIN, M. J. Teor de oxigênio no final de sopro nos convertedores LD da Usiminas. *Siderurgia*, São Paulo (50):25-30, 1974.

21. MUSETTI, A. & HERTWIG, I. O. Desoxidação e tratamento do aço sob vácuo. *Metalurgia*. São Paulo, 28:841-55, 1972.

22. ROBERTS, L. E. & HARPER, E. A. *The determination of oxygen in uranium oxides.* Harwell, Berks., Atomic Energy Research Establishment, May 1952. (AERE-C/R-885).

23. STONHILL, L. G. The determination of atomic ratios in the uranium-oxygen system by a thermogravimetric method. *Can. J. Chem.*, Ottawa, 37:454-9, 1959.